J Mater Sci (2006) 41:5576–5586
DOI 10.1007/s10853-006-0334-y

Texture evolution during deformation of an Al-6%Cu-0.4%Zr superplastic alloy

M. Eddahbi · M. Carsí · O. A. Ruano

Received: 16 June 2004 / Accepted: 15 September 2005 / Published online: 20 June 2006

Abstract Texture measurements of the as-received rolled Al-6%Cu-0.4%Zr alloy revealed that a copper component, {311}<233>, is developed at the surface and a S component, {631}<113>, is formed at the middle of the sheet. During early stages of superplastic deformation at 480 °C/ 5×10^{-4} s^{-1} the intensity of the Cu component increases slightly whereas the S component changes toward the brass component Bs, {110}<112>, by a slip process. For larger strains, both components decrease by a grain boundary sliding mechanism.

Introduction

Limiting the microstructural characterization, exclusively, to the determination of size and shape of grain and second phase particles, may result in an erroneous description and interpretation of the nature of the mechanism controlling deformation processes. The introduction of texture measurements in the analysis of materials has permitted to obtain further intrinsic microstructural aspects which are not identified by common conventional techniques [1–6] This analysis has allowed to clarify some ambiguities on the nature of processes controlling the evolution of the microstructure during annealing and/or deformation [7, 8].

Another gain obtained from the introduction of the texture analysis is the determination of texture gradients throughout a rolled sheet [9, 10]. These gradients, on the other hand, are known to influence the mechanisms governing the high temperature deformation of some materials [11–15].

It has been demonstrated that ultrafine-grained structures can be obtained in a series of aluminium alloys containing Zr, Cr or Sc, and these alloys have attracted considerable interest because of their superplastic forming capability [16–18]. These based Al-alloys may be superplastically deformed in one of two microstructural conditions: a fully recrystallized condition and a cold or warm rolled condition. In the second case, an interesting structural aspect of such alloys is that prior to superplastic deformation (SPD) they can generally be classified as not recrystallized. It was reported for an Al-6%Cu-0.5%Zr alloy that a fine grained structure is obtained during early stages of SPD as a result of strain induced continuous recrystallization [19–21]. This mechanism occurs by conversion of a subgrain structure to a high angle grain structure.

In materials having a texture gradient it is expected that various recrystallization and deformation mechanisms may occur during deformation. The aim of this study is to describe the global microstructural changes (grain structure and texture) during SPD of an Al-6%Cu-0.4%Zr alloy. Special attention will be paid to the texture gradients effects on the superplastic behavior of such alloy.

Experimental procedure

The Al-6%Cu-0.4%Zr (nominal composition in wt.%) alloy was provided in the form of a 3 mm thick sheet. Tensile specimens were machined from the as-processed rolled sheet such that the tensile axis was parallel to the rolling direction.

M. Eddahbi (✉) · M. Carsí · O. A. Ruano
Departamento de Metalurgia Física, Centro Nacional de Investigaciones Metalúrgicas, CSIC,
Avda. de Gregorio del Amo 8, 28040 Madrid, Spain
e-mail: eddahbi@cenim.csic.es

Texture measurements were carried out by measurement of pole figures in the Schulz reflection method, using a Siemens diffractometer equipped with a D5000 goniometer and an open Eulerian cradle. Incomplete pole figures {111}, {200}, {220} and {113} were measured over a range of azimuthal angles χ from 0° to 75° in the step mode with increments of $\Delta\chi = \Delta\phi = 5°$. A textureless standard sample of pure aluminium was used for defocusing correction. Quantitative three-dimensional orientation distribution functions (ODF) were obtained using the series expansion method ($l_{max} = 22$) [22]. The ODF were represented with iso-intensity lines in equidistant sections, $\Delta\phi_2 = 5°$, through the Euler's space defined by ϕ_1, Φ and ϕ_2 angles.

Texture measurements were carried out on the rolling plane (RD/TD plane) at both the surface and the middle plane of the samples, using the conventional reference system R_A (RD,TD,ND). In addition, texture measurements were also carried out on the ND/TD plane employing the reference system R_B (TD,ND,RD) as illustrated in Fig. 1. The use of this reference system allows a complete description of the global texture throughout the rolled sheet [23]. In addition, only one measurement is sufficient to describe the global texture using the system R_B whereas two measurements are necessary in the conventional system.

The grain structure was revealed by both Keller and Barker reagents. Optical microscopy was used to characterize the microstructure in the rolled, annealed and deformed state.

Results

As-processed material

Fig. 2a shows ϕ_2 sections of the ODF of the as-processed material obtained on the RD/TD plane (system reference R_A in Fig. 1). The data recorded correspond to the surface of the sheet. The texture can be described by orientations constituting the β-fiber, i.e., copper {311}<233> (Cu), {123}<523> (S) and brass {110}<112> (Bs) components. It is observed that the intensity maximum is located at the Cu component. As an approach, the global texture of the as-received material at the surface can be described by a combination of Cu orientation and its symmetric respect to the TD direction as shown in Fig. 4a.

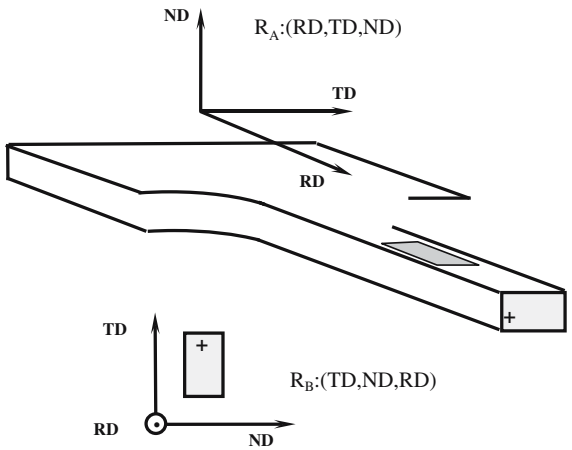

Fig. 1 Schematic illustration of the conventional reference system R_A and the reference system R_B employed for texture measurements

Fig. 2b shows ϕ_2 sections of the ODF corresponding to the middle of the as-processed material obtained on the RD/TD plane (R_A system in Fig. 1). It is observed that the texture is different from that obtained at the surface. It consists of a fiber texture, named *x-fiber*, that extends from the orientation {021}<123> (A) at $\phi_2 = 0°$ to the orientation {321}<235> (S″) at $\phi_2 = 20°$. The maximum of the intensity is located at the {631}<113> orientation at $\phi_2 = 15°$ which is close to the {421}<112> (S) orientation. This orientation can also be detected at $\phi_2 = 35°$ and $\phi_2 = 65°$. Furthermore, for $\phi_2 = 45°$ it is evident that the Cu component is not developed and the {110}<111> (P) orientation, slightly rotated respect to the ND, is observed. As an approximation, the texture at the middle of the as-received material can be described by a combination of the four variants of the S component as illustrated in Fig. 4d.

Fig. 3 shows ϕ_2 sections of the ODF of the as-processed material obtained on the transverse plane (ND/TD plane) in the system reference R_B (Fig. 1). In this case, the scanned area may involve several layers through the thickness of the sheet and the data recorded may correspond to both the surface and the middle of the sheet thus providing more information. It is important to note that the displayed ODF was not corrected and corresponds to the reference system R_B. However, the components displayed in the ODF were corrected and correspond to the conventional system R_A. The texture is composed, principally, of the Cu and the S components as shown for $\phi_2 = 45°$ section in the figure. It can be demonstrated that a simple rotation of 90° around TD and ND brings the two systems reference, R_A and R_B, of Fig. 1 together.

Annealed material

Fig. 4 shows (111) pole figures on the RD/TD plane of the Al-6%Cu-0.4%Zr alloy in the as-received and annealed state (480 °C) at the surface and the centre of the rolled sheet. At the surface the annealing treatment does not led to a different texture and the main component (Cu) is maintained. However, the texture intensity first increases during early stage of annealing (480 °C/10 min) (Fig. 4b) and then decreases for further exposure time (480 °C/50 min)

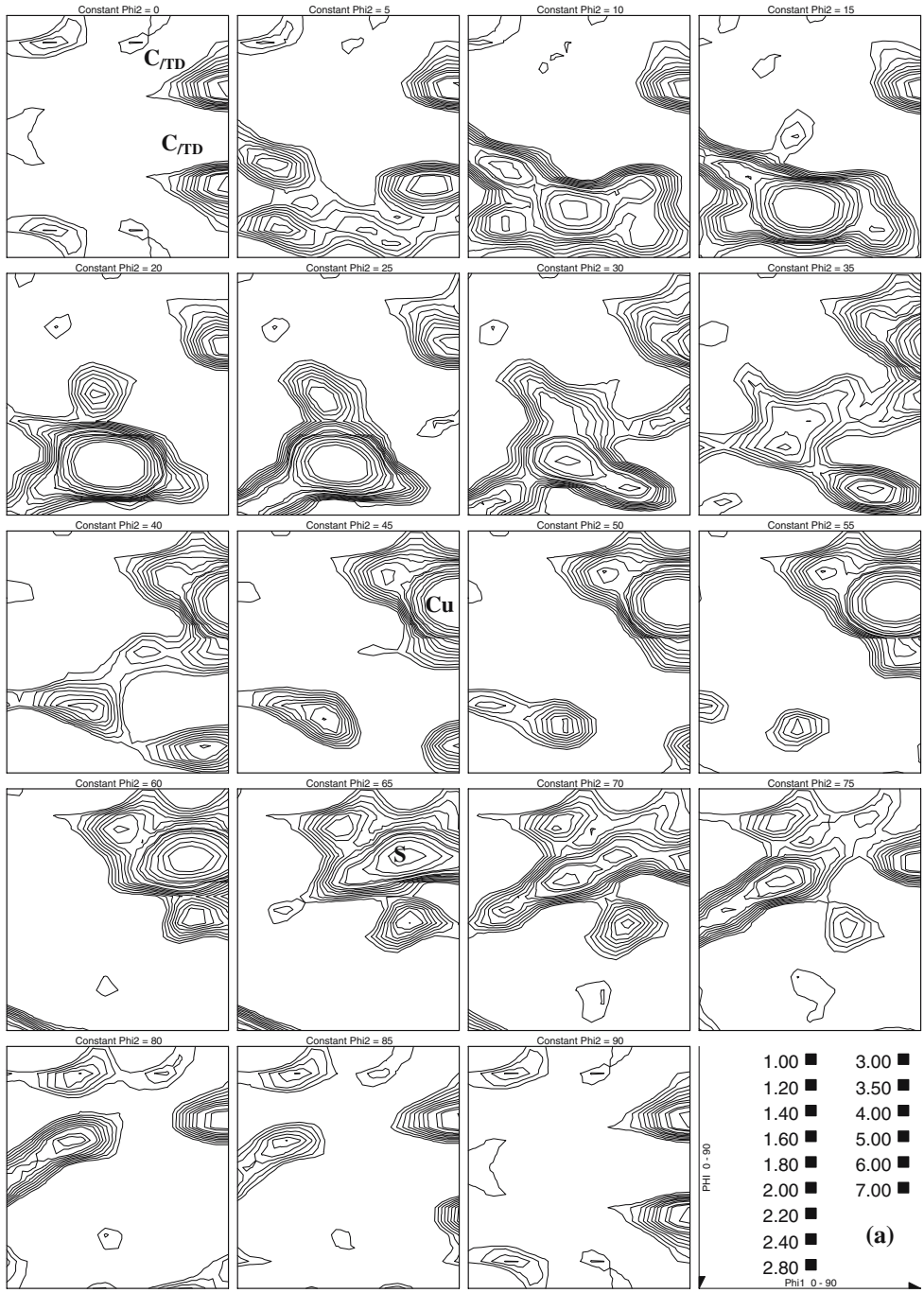

Fig. 2 Texture of the as-received Al-6%Cu-0.4%Zr alloy obtained on the rolling plane (RD/TD plane): (**a**) ODF at the surface of the sheet and (**b**) at the middle

as observed in Fig. 4c. At the middle of the sheet, Fig. 4e, the intensity of the main component (S) during a short annealing time, 480 °C/10 min, is maintained unchanged with respect to the as-received state, Fig. 4d. For larger annealing time, 480 °C/50 min, the (111) pole intensity of the S component decreases and a tendency towards the P and/or Bs (hereafter noted as P-Bs) orientations is observed as shown in Fig. 4f. It is worth to note the strong decrease of the (111) pole density, indicated by an arrow, and located at $\phi = 30°$ from the ND toward the RD.

Superplastic deformation

Tensile tests were carried out at 480 °C and 5×10^{-4} s^{-1} at different true strains in order to show the evolution of the microstructure and the texture with strain. A sequence of strain rate jumps was performed at different strains during a single test to evaluate the strain rate sensitivity parameter (m). The results showed that the m value increased in the strain range of $\epsilon = 0$–0.7 from 0.3 to 0.5. At the steady state, extended between $\epsilon = 0.7$–1.2, the m value was constant at about 0.5. For larger strains ($\epsilon > 1.2$), it

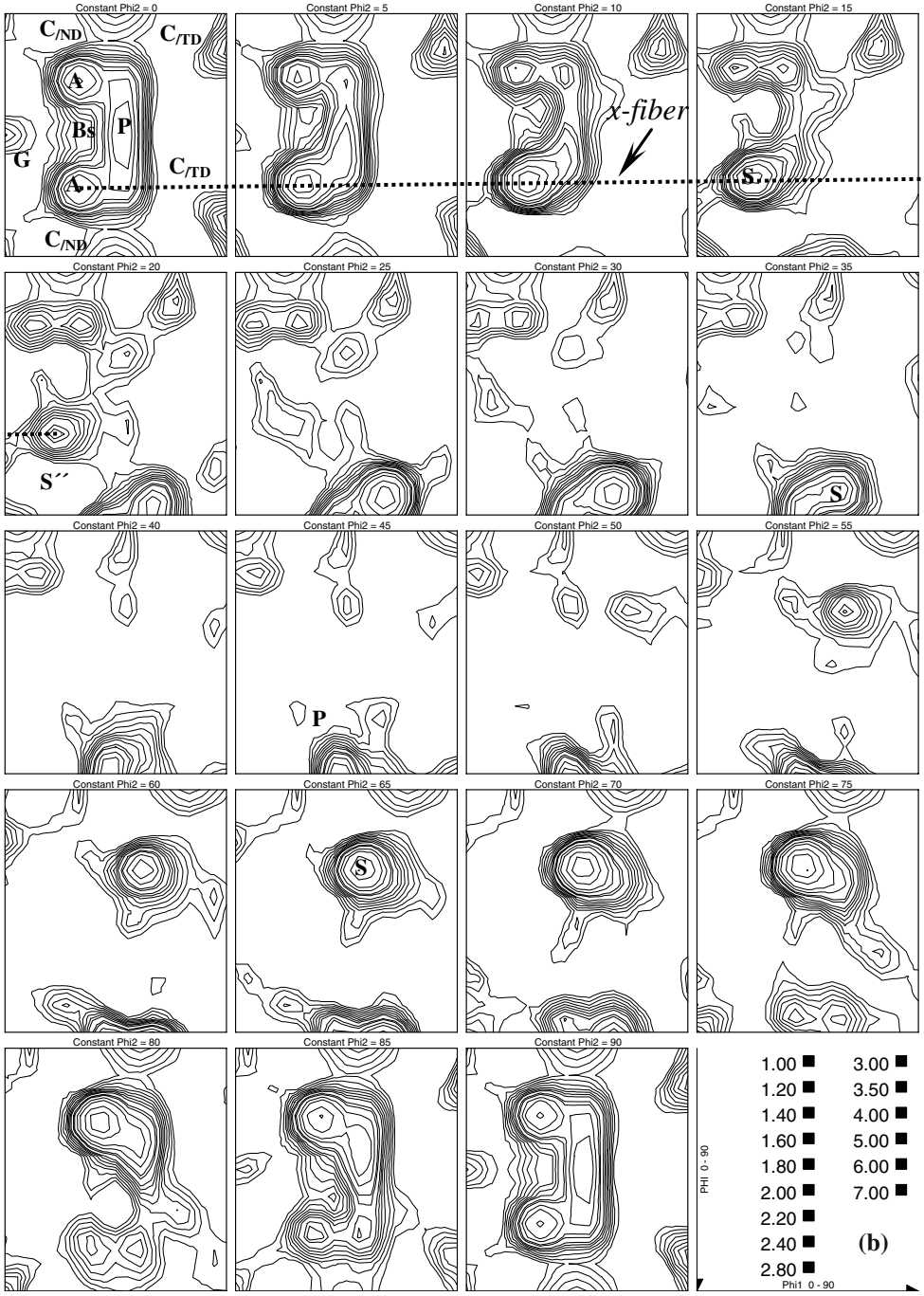

Fig. 2 continued

decreased to a low value of 0.3 [16, 24]. The variation of m with strain may reflect that microstructural changes had occurred during deformation.

Fig. 5 shows the ODF and the (111) pole figures obtained at both the surface and middle plane of a sample deformed to failure ($\epsilon = 1.5$) at 480 °C/5×10^{-4} s^{-1}. At the surface of the deformed sample, Fig. 5a and b, the texture intensity of the main component (Cu) decreases, compared to that of the as-received state in Fig. 2a. However, the most relevant issue arising from this analysis is that such component is maintained even after large strains at high temperature. Furthermore, orientation dispersion around the TD can also be observed.

The texture measured at the middle plane of the deformed sample, displayed in Fig. 5c and d, reveals that the *x-fiber* orientations observed in the as-received state, and marked with a dashed line in the figure, disappears

and a new fiber, called *y-fiber* and marked with a continue line, is developed. This fiber extends from the P-Bs orientations at $\phi_2 = 0°$ to the Cu orientation at $\phi_2 = 20°$. This indicates that an orientation change had occurred during deformation resulting in the formation of the Bs component at the expenses of the disappearance of the S component.

The microstructure of the Al-6%Cu-0.4%Zr alloy in the as-received, annealed and deformed states are shown in Fig. 6. Fig. 6a corresponds to the as-received material obtained on the longitudinal plane (ND/RD plane). It is shown that the microstructure is heavily deformed inside the bands, 0.5–1 μm in thickness, along the ND on the ND/RD plane, and aligned with the rolling direction. After annealing at 480 °C/30 min, recrystallization is observed as shown in Fig. 6b. Some coarse grains and traces of the banded structure, containing small (sub)-grains, are still evident. After straining at 480 °C/5×10^{-4} s^{-1} to $\epsilon = 0.4$ some traces of the banded structure are present but new (sub)grains are developed as shown in Fig. 6c. In contrast, at larger strains (Fig. 6d) the (sub)grains become equiaxic.

Discussion

It is well known that superplasticity requires small recrystallized grains and high angle grain boundaries to support grain boundary sliding (GBS), mechanism that characterizes the SPD. It is evident that the microstructure

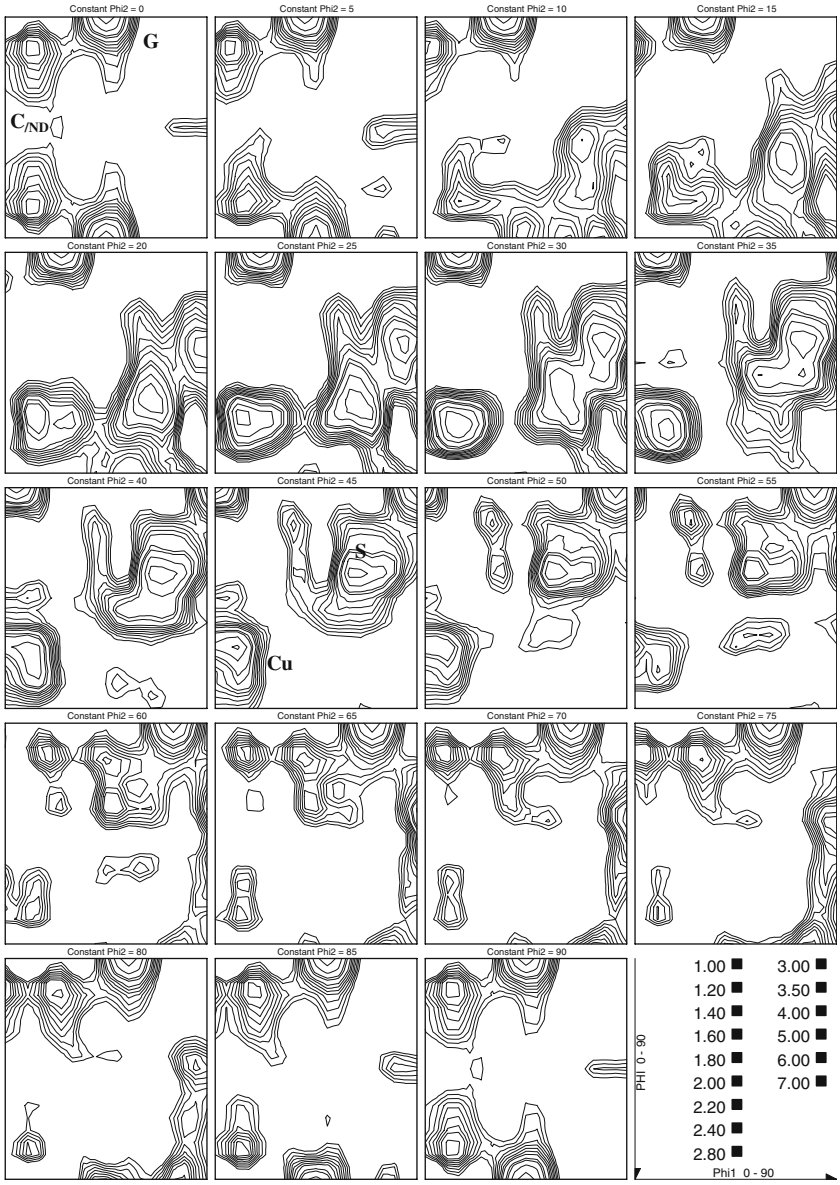

Fig. 3 ODF of the as-received Al-6%Cu-0.4%Zr alloy obtained on the transverse plane (TD/ND plane)

of the as-received rolled Al-6%Cu-0.4%Zr alloy (Fig. 6a) is not favorable for GBS since it is a deformed banded grain structure containing (sub)grains [16, 24]. It was recognized that some alloys, particularly the Al-alloys, may be superplastically deformed in one of two microstructural conditions: a fully recrystallized condition and a cold/warm rolled condition. The second condition corresponds to the alloy investigated in this study. The unrecrystallized microstructure transforms during early stages of deformation (up to about a true strain of 0.7) into small recrystallized (sub)grains [24]. The energy stored as a heavily deformed substructure is the main driving force for a recrystallized microstructure able to show SPD. This cold rolled condition offers an important structural advantage compared to the fully recrystallized condition since fine (sub)grain size can be obtained.

The true stress versus true strain curve of the cold rolled Al-6%Cu-0.4%Zr alloy tested at 480 °C/5×10^{-4} s^{-1} exhibited three deformation stages, I, II and III, as described elsewhere [24]. Work hardening occurred in stages I and III where the strain rate sensitivity value, *m*, was low (about 0.3) and a nearly steady state behavior was observed in stage II where *m* took a constant value of 0.5. This variation of *m* with strain during the tensile test indicates that changes of the grain structure and the texture occur in each of the three deformation stages. For texture determination, measurements were carried out, separately, on the RD/TD plane in the conventional system (R_A)

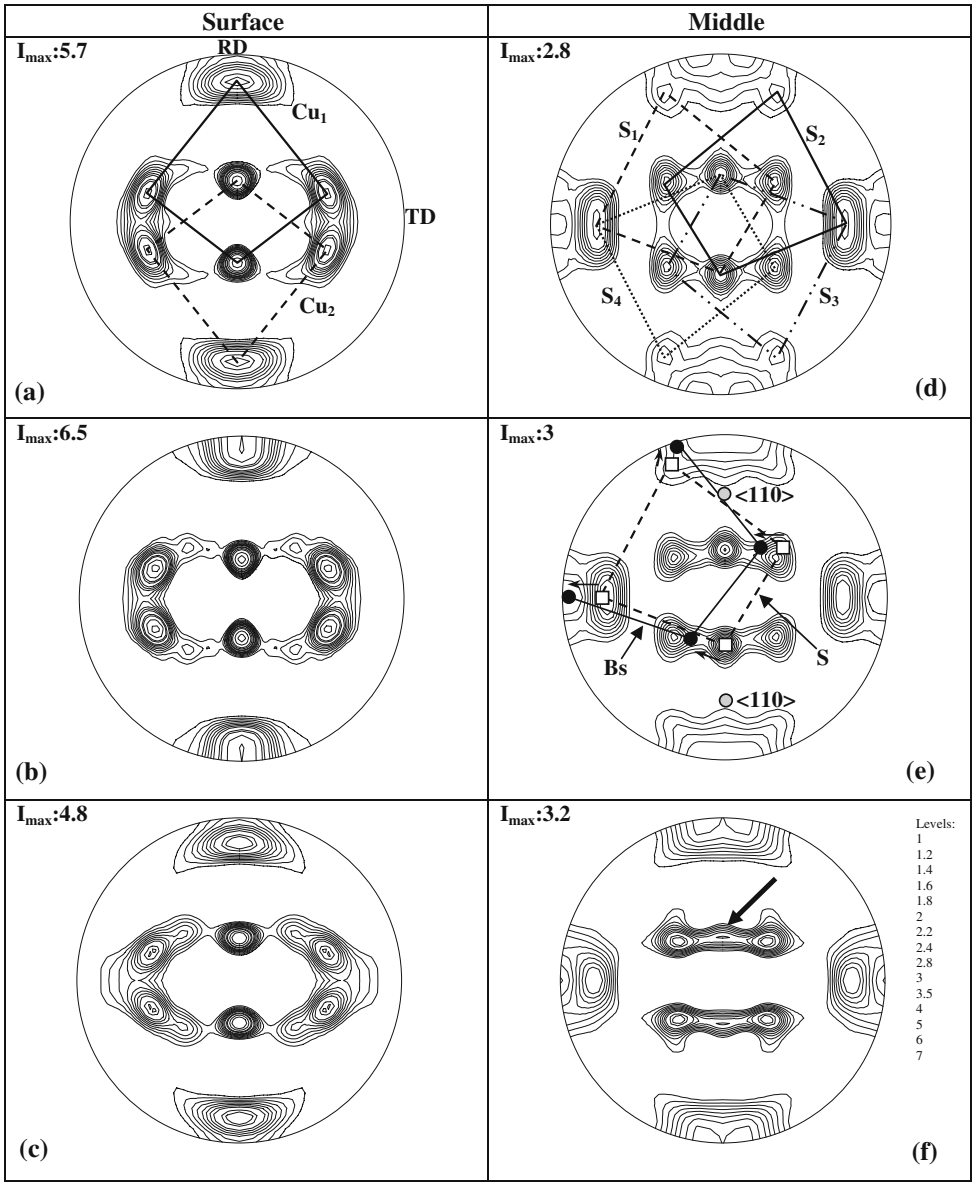

Fig. 4 (111) pole figures of the Al-6%Cu-0.4%Zr alloy obtained on the rolling plane (RD/TD plane): (**a**), (**b**) and (**c**) at the surface in the as-received state, annealed at 480 °C/10 min and 480 °C/50 min, respectively. (**d**), (**e**) and (**f**) at the middle of the sheet in the as-received state, annealed at 480 °C/10 min and 480 °C/50 min, respectively. The intensity levels given in (**f**) correspond also to the other pole figures

(Fig. 2) and on the TD/ND in the system R_B (Fig. 3). It is observed that the texture on the latter system (R_B), which is not commonly used, is the same as in the conventional system R_A. It is worth noting that the use of the R_B system (TD/ND plane in Fig. 3) for texture measurements is of great importance since it allows determination of the texture along the thickness of the sample. This helps to elucidate the nature of the mechanisms responsible of the global microstructural changes taking place during annealing and/or deformation. It is observed in Fig. 2a that the texture measured at the surface of the rolling plane (RD/TD plane) can be described by the Cu component. In contrast, at the middle of the sheet, the S component is developed as observed in Fig. 2b. It is evident, therefore, that a gradient of texture is formed through the thickness of the as-received rolled sheet.

The development of different rolling textures at different through-thickness layers of the sheet has been associated in the literature to various effects. Friction between the roll and the sheet surface, temperature gradient through the thickness during rolling pass, geometrical changes during the rolling passes and the geometry of the rolling gap have been considered to be the principal parameters influencing the final microstructure [25–27]. Globally, it is expected that the texture gradient in the Al-6%Cu-0.4%Zr alloy should be caused by the non-uniformity of the penetration of the shear deformation through the thickness of the material during rolling. In this study we will not address the issue of the origin of the gradient texture in this alloy because we are interested in the texture evolution of such alloy having initially a texture gradient.

In the annealed state (480 °C/10 min) the intensity of the Cu component, at the surface, increases whereas that of the S component, at the middle, is somewhat constant as shown in Fig. 4. This change is accompanied by a decrease in orientation dispersion observed along the fibers in the ODF displayed in Figs. 2 and 3. The increase in the intensity of the Cu component is ascribed to a recovery process as discussed in a previous work [16, 24]. In other words, a reorientation of the microstructure, due to slight rotation of low misoriented (sub)grains and/or deformed cells with a Cu orientation, occurs at the surface of the annealed sample. It is expected that this annealing

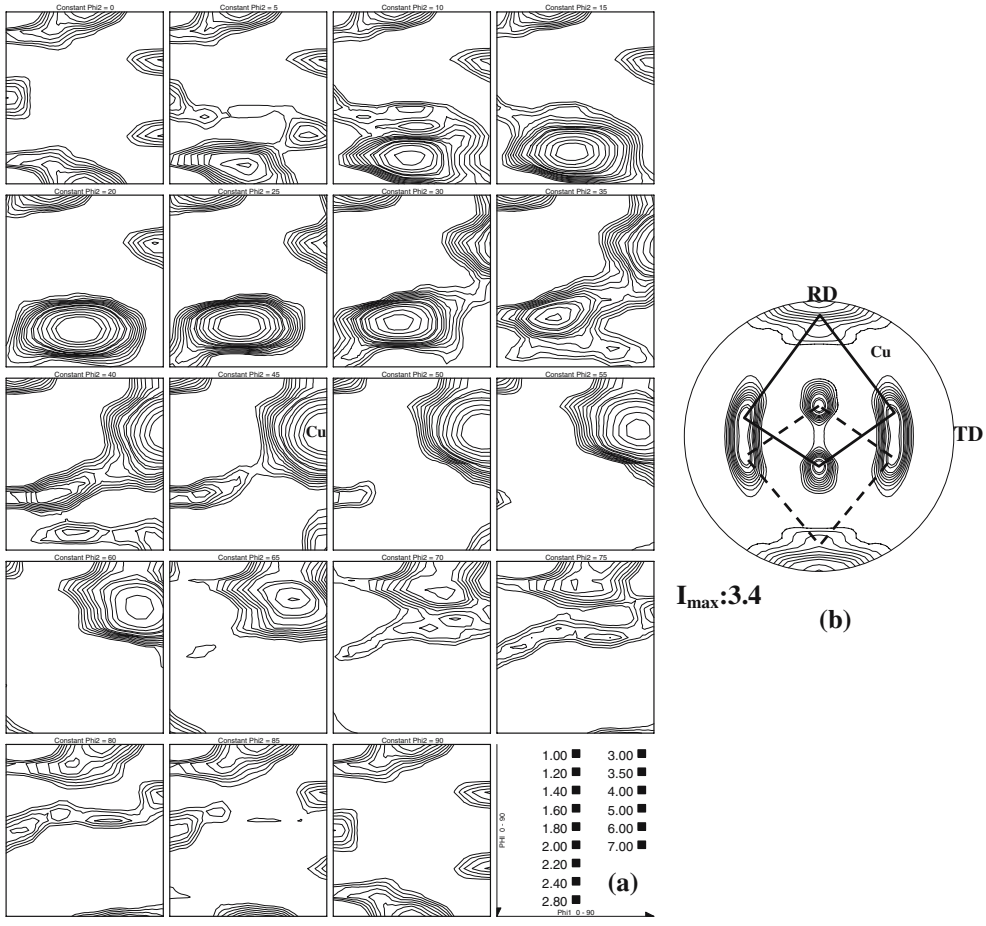

Fig. 5 Texture of the Al-6%Cu-0.4%Zr deformed to $\epsilon = 1.4$ at 480 °C/5×10^{-4} s^{-1}: (**a**) and (**b**) ODF and (111) pole figures, respectively, corresponding to the surface of the sample, (**c**) and (**d**) ODF and (111) pole figures, respectively, corresponding to the middle of the sample. The main components are indicated

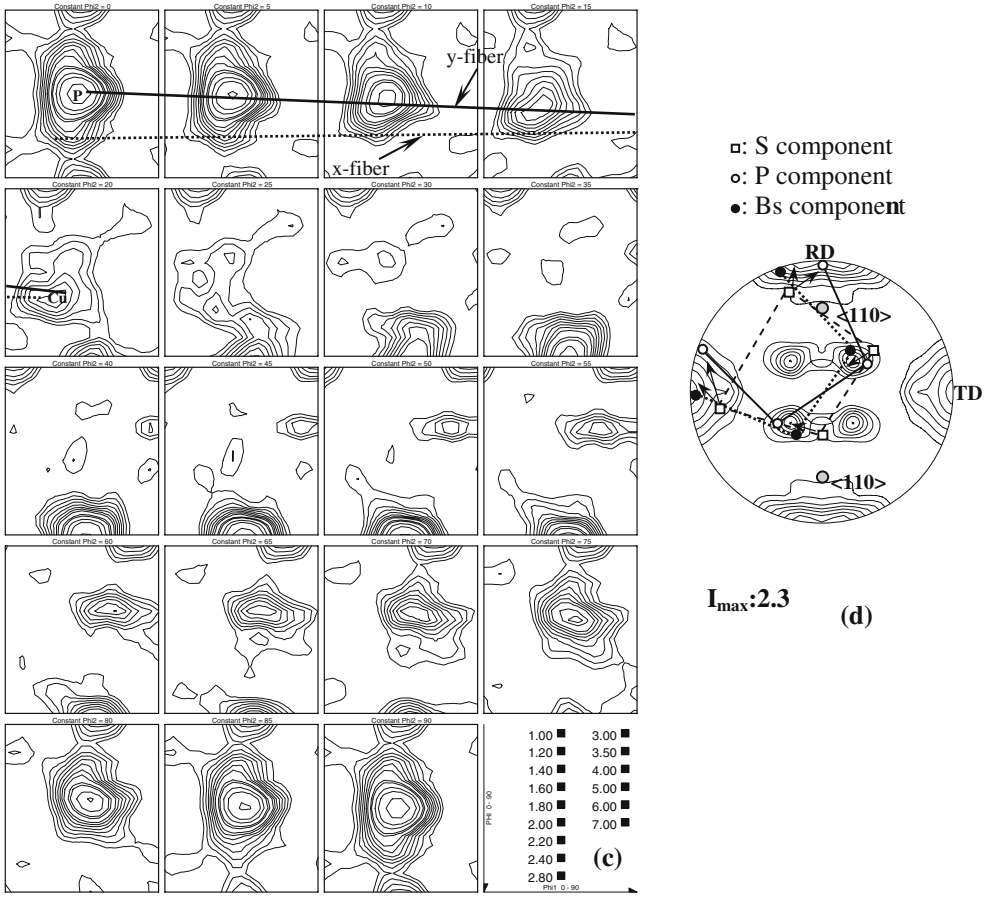

Fig. 5 continued

process, or continuous recrystallization, may induce an increase of the misorientation angle. For large exposure annealing treatments at 480 °C/50 min, the typical recrystallization textures, such as the cube, {100}<001> and/or the Goss, {110}<001> textures, are not observed neither at the surface nor at the center of the sheet. Instead, the intensity of the Cu component decreases at the surface due to grain coarsening (Fig. 4c) whereas, the intensity of the S component slightly decreases at the middle of the sheet and the orientation density close to the P-Bs orientations increases. This can be interpreted as the disappearance of the S component at expenses of the P-Bs orientations. An explanation of this behavior can be given considering that at the middle of the as-received rolled sheet the adjacent layers can be described mainly by a coexistence of two kinds of (sub)grains, some oriented close to the S orientation and others close to the P-Bs orientations. This (sub)grain rearrangement could lead a (sub)grain Bs to be in contact with at least a (sub)grain of one variant of the S component. In such case, an orientation relationship $\theta°<110>$ should exist as illustrated in Fig. 4e by means of pole figures of the variants of S and Bs. It is shown that these two variants may be brought into coincidence by a rotation of $\theta = 25°$ around the <110> pole. On the basis of these assumptions, it is expected that the boundaries $\theta°<110>$ possess a high mobility that allow them to swipe the adjacent S (sub)-grains. Therefore, an oriented grain growth process may explain the evolution of the microstructure and texture during annealing of the Al-6%Cu-0.4%Zr alloy at the middle of the sheet [28].

On the other hand, the recrystallized microstructure of the annealed material shows the coexistence of small and coarse grains as shown in Fig. 6b. It is observed that the annealing treatment gives rise to an inhomogeneous microstructure in grain size and shape which should be deformation and orientation dependent. It is suggested that the coarse grains are originated at the deformation zones close to the Al_2Cu particles which are potential sites for recrystallization as well as at $\theta°<110>$ boundaries [8, 29–31]. Both contribute to abnormal grain growth, i.e., secondary recrystallization.

During SPD at 480 °C/5×10^{-4} s^{-1} no new components are developed through the full thickness of the deformed

samples. The intensity of the Cu component at the surface of the sheet increases during the first stages of straining which can be ascribed to extended dynamic recovery and formation of small (sub)grains. With further deformation, the intensity decreases continuously. This is attributed to the operation of a GBS mechanism that generally leads to texture weakening [32, 33]. At the middle of the sheet, however, it is approached that the S component reorients during deformation towards the P-Bs orientations by continuous rotation around the <110> axis as illustrated in Fig. 5d. This assumption is supported on the basis that the S orientation is unstable under special conditions as previously reported [3]. Thus, the S orientation may rotate along the β-fiber toward either the Cu or the Bs orientation. Consequently, it is suggested that a slip process occurs at the middle of the sample from the beginning of deformation up to a strain where all the (sub)grains, initially with the S orientation, are transformed into the Bs orientation. The orientation changes can be estimated comparing the ODF of both the as-received material (Fig. 2b) and the superplastically deformed material that was deformed to $\epsilon = 1.4$ at 480 °C/5×10^{-4} s^{-1} (Fig. 5c). It is observed that the *x-fiber* orientations, initially extended from the orientation A at $\phi_2 = 0°$ to near the S″ orientation at $\phi_2 = 20°$, changes toward the *y-fiber* orientations, that are extended from the P orientation at $\phi_2 = 0°$ to the Cu orientation at $\phi_2 = 25°$ as shown in Fig. 5c. Furthermore, the A component observed at the middle of the as-received sheet disappears during deformation and an orientation dispersion around the P-Bs orientation is noted in Fig. 5c at $\phi_2 = 0°$ (compare Figs. 2b and 5c for $\phi_2 = 0°$). On the other hand, the presence of the $\theta° < 110>$ misoriented boundaries, as mentioned before, let us expect that, in addition to slip and GBS process, some grain boundaries migration should take place during deformation. Therefore, it is concluded that the superplastic behavior of this alloy, initially containing a gradient of texture, is not simple as observed in other conventional superplastic alloys. In other terms, the GBS is not the unique process in the entire deformation range and slip and grain boundary migration may operate simultaneously and/or successively during deformation.

The microstructural changes at both the surface and the middle of the deformed material can be interpreted in terms of changes of *m* with strain. At the beginning of stage I the *m* value is close to 0.3 indicating that slip controls deformation. However, as the stage II is approaching the *m* value increases to 0.5 indicating that the contribution of GBS has increased with strain. During stage II, the banded structure is further fragmented (Fig. 6c and d) and the strain rate sensitivity is maintained constant at about 0.5. Similar trends were observed to occur in Al–Li alloy under SPD conditions [19]. The intensity of the Cu component is further decreasing by GBS at the surface. In turn, at the

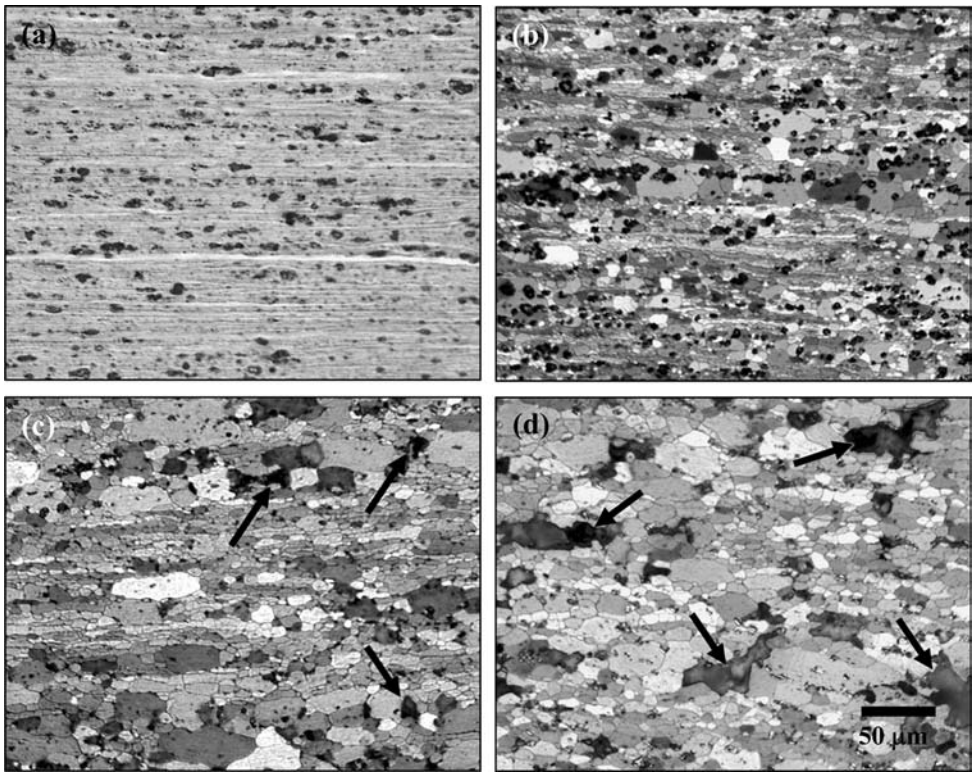

Fig. 6 Microstructures on the transverse plane of the Al-6%Cu-0.4%Zr: (**a**) As-received, (**b**) annealed at 480 °C/30 min, (**c**) deformed to $\epsilon = 0.4$ and (**d**) deformed to $\epsilon = 1.2$. The scale given in (**d**) corresponds to the other micrographs and the arrows indicate the cavities

middle, it is proposed that part of the (sub)grains, which still had S orientation, transforms toward the Bs orientation by slip whereas the (sub)grains that have been rotated to Bs deform by GBS. For strain larger than $\epsilon = 0.7$, (Fig. 6d) the banded structure of the as-received state totally disappears and the global texture intensity weakens which proves that GBS controls deformation in the entire volume of the sample.

It is worth noting that the microstructural changes during SPD of the Al-6%Cu-0.4%Zr alloy are accompanied by cavities formation indicated by arrows in Fig. 6c and d. This damage process affects seriously the material properties and limits its ductility. Particularly, it was shown that the formation of the cavities during deformation obstructs the GBS mechanism in the superplastic materials [16, 34–36]. The formation of these defects can be ascribed to many factors but the most relevant is linked to the presence of second phase particles located, principally, at the grain boundaries and triple junctions. It was observed that decohesion at the interface between the particles and the matrix was the origin of the cavities. In the current study, in addition to the presence of Al_2Cu particles, it is suggested that the texture gradient present in this alloy may induce the formation of cavities during SPD. It can be assumed that the deformation behavior and/or the stress state manifested by the grains with a Cu texture at the surface of the sample may be different and independent from that occurring at the middle. This difference in behavior may induce microstructural heterogeneities resulting in the formation of cavities.

Conclusions

1. The as-received Al-6%Cu-0.4%Zr alloy shows texture gradients through the thickness of the rolled sheet, a Cu component, $\{311\}<233>$, at the surface and a S, $\{631\}<113>$, component at the middle.
2. During annealing at 480 °C/50 min, the initial microstructure recrystallizes without formation of the cube and the Goss textures, typical recrystallization textures in Al-alloys. At the surface of the sheet, the intensity of the Cu component decreases whereas, at the middle, the S component decreases at the expense of the P-Bs orientations. A $\theta°<110>$ orientation relationship between the S and the P-Bs orientations is proposed to explain the change of the grain structure and the texture during annealing at the middle of the sheet.
3. During the early stages of deformation ($\epsilon < 0.7$), the initial banded structure fragments to form a recrystallized microstructure. At the surface of the sheet the Cu component increases slightly and then decreases continuously. Simultaneously, the S component changes towards the Bs component at the middle of the sheet. It is suggested that, in this deformation range, GBS controls deformation at the surface of the sample whereas, at the middle both slip, grain boundary migration and GBS are taking place. For larger strains ($\epsilon > 0.7$), the intensity of both components decreases indicating that GBS mechanism controls deformation in the full thickness.
4. The cavities formed during SPD may be induced by the texture gradients through the thickness of the alloy.

Acknowledgements The authors gratefully acknowledge the support of the *Comisión Interministerial de Ciencia y Tecnología (CICYT)* under Grant MAT2003-1172 and MAT2000-2017. One of the authors (M Eddahbi) thank the Grant *345/2000* from the *Comunidad Autónoma de Madrid.*

References

1. Hirsch J, Lücke K (1988) Acta Metall 36:2883
2. Engler O, Hirsch J, Lücke K (1989) Acta Metall 37:2743
3. Hirsch J (1990) Mater Sci Technol 6:1048
4. Lücke K, Engler O (1990) Mater Sci Technol 6:1113
5. Lee CS, Duggan BJ (1993) Acta Metall Mater 41:2691
6. Ren B, Morris JG (1995) Metall Trans 26A:31
7. Bowen AW (1990) Mater Sci Technol 6:1058
8. Doherty D, Hughes DA, Humphreys FJ, Jonas JJ, Jensen DJ, Kassner ME, King WE, Mcnelley TR, Mcqueen HJ, Rollet AD (1997) Mater Sci Eng 238A:219
9. Kashyap BP, Fan W, Chaturvedi MC (2001) Mater Sci Technol 17:248
10. Gourdet S, Montheillet F (2000) Mater Sci Eng 283A:274
11. Kalu PN (1993) In: Jonas JJ, Bieler TR, Bowman KJ (eds) Advances in hot deformation textures and microstructures, Pittsburgh. TMS publications, p 349
12. Pérez-Prado MT, Cristina MC, Torralba M, Ruano OA, Gónzalez-Doncel G (1996) Scripta Mater 35:1455
13. Blackwell PL, Bate PS (7–8 December 1994) In: Norman Ridley (ed) 60 years after Pearson, Proceedings of the Conference on Superplastic Forming, London,The Institute of Materials p 183
14. Blackwell PL, Bate PS (1993) Metall Trans 24A:1085
15. Barlat F, Brem JC, Liu J (1992) Scripta Metall Mater 27:1121
16. Eddahbi M (1998) Ph.D, Thesis, Universidad Complutense de Madrid
17. Padmanabhan KA, Hirsh J, Lücke K (1991) J Mater Sci 26:5309
18. Martin CF, Blandin JJ, Salvo L (2001) Mater Sci Eng 297:212
19. Qing L, Xiaoxu H, Mei Y, Jinfeng Y (1992) Acta Metall Mater 40:1753
20. Sakai T, Yang X, Miura H (1997) Mater Sci Eng A234–236:857
21. Matsuki K, Iwaki T, Tokizawa M, Murakami Y (1991) Mater Sci Technol 7:513
22. Bunge HJ (1982) Texture analysis in materials science, Butterworths
23. Inoue H, Takasugi T (2001) Z Metallkd 92:82
24. Eddahbi M, Mcnelley TR, Ruano OA (2000) Metall Trans 32A:1093
25. Kuo VWC, Starke EA, Jr. (1985) Metall Trans 16A:1089
26. Engler O, Sachot E, Ehrström JC, Reeves A, Shahani R (1996) Mater Sci Technol 12:717

27. Fan W, Kashyap BP, Chaturvedi MC (2001) Mater Sci Technol 17:431
28. Matsuki K, Uetani Y, Yamada M, Murakami Y (1976) Met Sci 10:235l
29. Humphreys FJ (1977) Acta Metall 25:1323
30. Humphreys FJ (1979) Acta Metall 27:1801
31. Humphreys FJ (2000) Scripta Metall Mater 43:591
32. Lee EW, Mcnelley TR (1987) Mater Sci Eng 93A:45
33. Ridley N (1990) Mater Sci Eng 6:1145
34. Sohal GS (1988) Mater Sci Technol 4:811
35. Jiang XG, Earthman JC, Mohamed FA (1994) J Mater Sci 29:5499
36. Padmanabhan KA, Engler O, Lücke K (1996) J Mater Sci 31:3971
37. Mizera J, Driver JH (1999) Mater. Sci. Eng. A271:334